Published in IET Radar, Sonar and Navigation
Received on 2nd April 2014
Revised on 23rd July 2014
Accepted on 26th July 2014
doi: 10.1049/iet-rsn.2014.0292

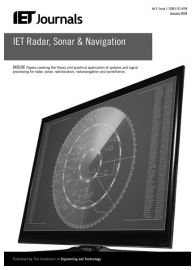


ISSN 1751-8784

# Radiolocation and tracking of automatic identification system signals for maritime situational awareness

*Francesco Papi[1], Dario Tarchi[1], Michele Vespe[1], Franco Oliveri[1], Francesco Borghese[2], Giuseppe Aulicino[3], Antonio Vollero[3]*

[1]*European Commission, Joint Research Centre (JRC), Institute for the Protection and Security of the Citizen (IPSC), Maritime Affairs Unit, Via Enrico Fermi 2749, 21027 Ispra (VA), Italy*
[2]*Elman s.r.l., Via di valle Caia km 4.7, Pomezia (Rome), Italy*
[3]*Italian Coast Guard Headquarters, Viale dell'Arte 16, Rome, Italy*
*E-mail: michele.vespe@jrc.ec.europa.eu*

**Abstract:** The automatic identification system (AIS), a ship reporting system originally designed for collision avoidance, is becoming a cornerstone of maritime situational awareness. The recent increase of terrestrial networks and satellite constellations of receivers is providing global tracking data that enable a wide spectrum of applications beyond collision avoidance. Nevertheless, AIS suffers the lack of security measures that makes it prone to receiving positions that are unintentionally incorrect, jammed or deliberately falsified. In this study, the authors' analyse a solution to the problem of AIS data verification that can be implemented within a generic networks of ground AIS base stations with no need for additional sensors or technologies. The proposed approach combines a classic radio-localisation method based on time difference of arrival with an extended Kalman filter designed to track vessels in geodetic coordinates. The approach is validated using anonymised real AIS data collected by multiple base stations that partly share coverage areas. The results show a deviation between the estimated origin of detected signals and the broadcast position data in the order of hundreds of metres, therefore demonstrating the operational potential of the methodology.

## 1 Introduction

The verification of the trustworthiness of automatic identification system (AIS) data is becoming a key problem to exploit the full potential of this technology not only for safety but also for security applications. AIS, originally conceived for collision avoidance, is a system whereby ships broadcast their presence, identification and location. Differently to other operational coastal active systems for maritime surveillance, AIS is characterised by considerable coverage (very high frequency (VHF) propagation) together with a relatively accurate positioning (global navigation satellite system (GNSS)) performance [1]. Nevertheless, the cooperative nature of AIS and the lack of intrinsic security make it vulnerable to false or missing declarations.

Ships of 300 gross tons and upwards in international voyages, 500 tons and upwards for cargoes not in international waters and passenger vessels are obliged to be fitted with AIS equipment as regulated by the International Maritime Organisation (IMO) Safety of Life and Sea (SOLAS) [2]. Furthermore, all EU fishing vessels of overall length exceeding 15 m are also required to be fitted with AIS from May 2014 [3].

AIS reports encode state vector information such as latitude, longitude, speed over ground (SOG), course over ground (COG) as derived by the on-board GNSS receiver. Such information is broadcasted at a variable transmission rate depending on the vessel motion: as an example, the rate is increased up to a message every 2 s when the vessel is sailing at high speed or manoeuvring. In addition, every 6 min, vessels transmit their identification (IMO and maritime mobile service identity (MMSI) number, ship name and call sign), static (size, type of vessel, type of cargo etc.) and voyage related information (e.g. estimated time of arrival (ToA) and destination). Such information is manually set and therefore not fully reliable since more subject to errors if compared with positioning data [4].

With the advent of networked regional base stations (BSs) (e.g. the European SafeSeaNet or the Mediterranean AIS Regional Exchange System – MAREΣ), and satellite receiver constellations [5], the system progressively proved effective for maritime surveillance and traffic monitoring, enabling far-reaching applications such as traffic knowledge discovery, route prediction and anomaly detection. The latter can target particular low-likelihood motion trajectories ([6, 7]), alerts such as sailing in restricted areas, abrupt changes of direction (an extensive overview of these rules is presented in [8]) or anomalies related to wrong AIS message information either unintentional or deliberate such as 'spoofing'. As an example, false GNSS tracking information can be produced to simulate specific trajectories [9] or false AIS messages can be generated and transmitted at VHF as recently demonstrated in [10]. Such events, besides being potentially serious hazards to the safety of navigation especially in reduced visibility conditions, can also represent security threats by covering unauthorised activities at sea such as illegal movements of goods and people.

The detection of position reporting anomalies either linked to AIS transponder failures or because of deliberately falsified broadcast dynamic information can be approached in different ways. The correlation with additional sensors can be used to detect AIS data spoofing; such sensors could be coastal radars (see e.g. [11]), high frequency (HF) surface wave radars [12] or space-based synthetic aperture radar [13]. Nevertheless, the operational usability of such approaches depends on the availability and persistency of the data provided by such additional sensors. Similar considerations apply to data correlation using secondary reporting systems such as long range identification and tracking. Other approaches aim at increasing the trustworthiness of the transponder through the use of additional on-board instrumentation as investigated by [14].

In this paper, we consider a methodology that can be easily applied to the existing AIS network using the messages normally provided by the AIS-BSs. The idea is to combine ToA measurements from multiple AIS channels to determine time difference of arrival (TDoA) measurements. Then TDoAs are processed using a classic multilateration (MLAT) procedure [15] to estimate the vessel position with uncertainty at each time instant [16]. Similar approaches based on MLAT and wide area MLAT techniques have been widely used for air traffic surveillance using secondary surveillance radar mode *S* replies (e.g. [17]) leading to location errors in the order of a few metres (see e.g. [18]). Differently from such applications, the localisation accuracy that can be achieved using AIS messages is significantly poor as the Cramer–Rao lower bound of the ToA estimate using such transmissions is limited by a signal bandwidth that is <25 kHz. This is further analysed in the following sections. Moreover, being the proposed approach leveraging existing systems, the receiving BSs are separated by baselines of tens or even hundreds of kilometres, their number is critically limited to a few units and in principle *ad hoc* deployments are not envisaged. Finally, the VHF radio propagation is often characterised by ducting effects that help in extending the AIS reception far beyond the line-of-sight but also lead to additional uncertainty on the relationship between the message time of flight (ToF) and the actual emission location. All the above make MLAT in this context not sufficient to guarantee anti-spoofing operational requirements in terms of location accuracy and coverage areas. As a consequence, a further AIS emission tracking stage is needed after classic MLAT approaches, whereby radiolocation accuracy is improved through time integration by means of an extended Kalman filter (EKF) in geodetic coordinates. This is made possible in the maritime domain as a consequence the relatively slow and predictable manoeuvres of ships with respect to the AIS messages refresh rates.

This paper aims at demonstrating the feasibility of radiolocation of AIS emissions as the basis for future anti-spoofing and AIS verification applications based on anomaly detection techniques.

This paper is organised as follows: in Section 2 we briefly describe the Italian AIS network; in Section 3 we introduce the models for ToA and TDoA measurements, and discuss the effects of noise with a specific attention towards bias compensation. In Section 4, we define the TDoA-based MLAT procedure and discuss some localisation results for different AIS network configurations. The EKF for time integration in geodetic coordinates is discussed in Section 5 along with the tracking results from processing real AIS data collected by the Italian AIS network. Finally, conclusions and future directions are discussed in Section 6.

## 2 Italian AIS terrestrial network

Implemented in 2005 to fulfil the requirements of the directive 2002/59/EC of the European Parliament and of the Council of 27 June 2002, the Italian AIS network has been completely upgraded in 2012–2103, with the aim to comply with the most recent relevant guidelines and recommendations, such as the International Association of Marine Aids to Navigation

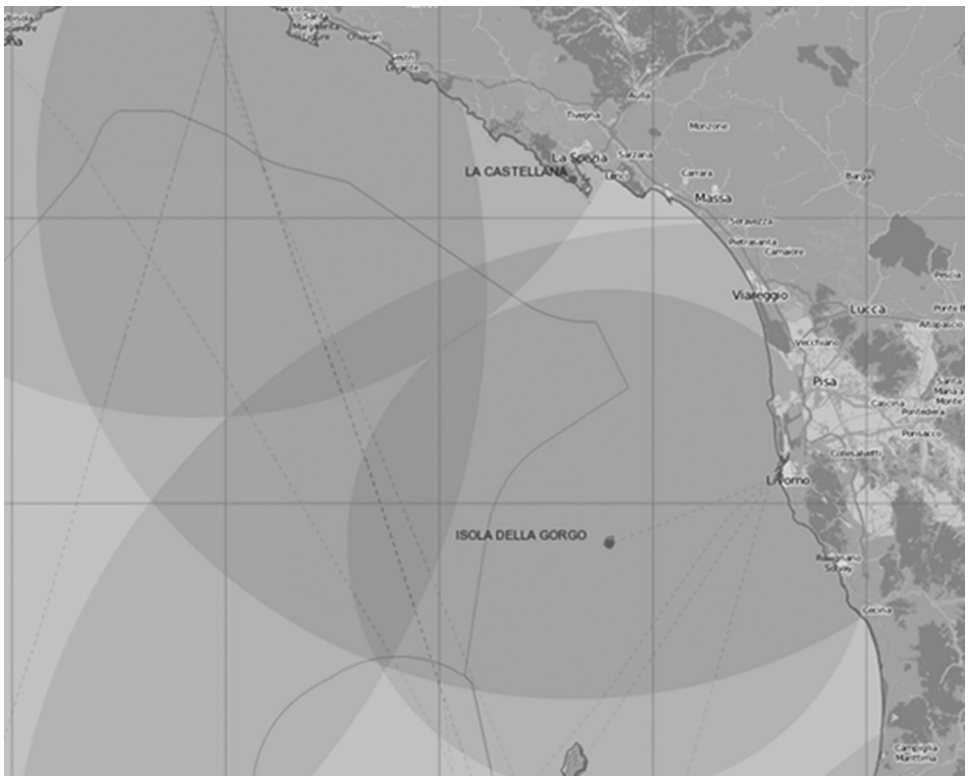


**Fig. 1** *AIS coverage overlapping*




doi: 10.1049/iet-rsn.2014.0292

and Lighthouse Authorities (IALA) Recommendation A 124 on 'The AIS Service' (December 2012) and the ITU Recommendation ITU-R M.1371–4 issued on April 2010. The network currently consists of 60 BSs mainly located to obtain the best VHF coverage (up to 100 nautical miles, even without the duct effect).

The BSs were placed in such a way to obtain an overlap of the radio coverage (Fig. 1) in order to: (i) increase the overall availability of the services provided by the national AIS network and (ii) enable future adoption of anti-spoofing techniques to improve quality of AIS information received. The overall architecture of the Italian AIS network is shown in Fig. 2. One of the key elements of the network is the so-called AIS embedded server, a fully solid-state device featuring two separate servers thus supporting redundancy or the simultaneous interface to two transmission control protocol (TCP) networks. The AIS embedded server, acting as a physical shore station (PSS) controlling unit according to the IALA Recommendation A-124, allows the integration of one or more BSs and their management from shore systems. The embedded server can acquire AIS data from the serial ports and from TCP connections according to the specified configuration.

In the same way, the collected AIS data are made available to serial ports and TCP connections. It also features an embedded interface for each web server which allows configuring and monitoring for both the servers and the connected AIS-BS, without using any additional software. Authorised operators can log-in on the web interface to configure and monitor every aspect of the server, its ports and connections and the linked devices and users.

The AIS system dynamically configures into cells using a self-organised time division multiple access scheme. The cell size is adjusted to adapt as a function of the traffic density: in highly congested areas for instance, it is necessary to reduce the size of the cell to diminish the number of transmitter in the cell; this is achieved by reducing the power of the AIS transponders from 12.5 W ('high setting') to 1 W ('low setting') thus avoiding message collisions [19]. AIS data are transmitted at a rate of 9.6 kb/s using Gaussian minimum shift keying (GMSK) modulation over two channels 161.975 and 162.025 MHz. For each channel, 2250 slots are allocated within a timeframe of 60 s, starting every minute. The bandwidth of the channels is nominally 25 kHz, although the AIS signal spectrum has to be within an emission mask defined by −25 dBc at +10 kHz and −70 dBc + 25 kHz [19]. Moreover, transmissions of AIS devices are synchronised by using a common time reference, UTC (coordinated universal time), provided by the internal GNSS receiver. Transmission timing error including jitter and systematic offsets should be within ±104 μs of the synchronisation source for mobile stations and ±52 μs for BSs, setting the limits of the accuracy of ToF estimation. If the internal GNSS receiver is faulty, the AIS devices are capable of synchronising to secondary timing sources as the received AIS messages; in this case, the timing error may increase up to 312 μs. Anyway, AIS stations are not allowed to discard received messages basing on timing error, even when it is much bigger than the above specified values.

## 3 ToA and TDoA measurements

In this section, we discuss the models used to describe ToA and TDoA measurements available from the Italian AIS network. Specific attention is devoted to the analysis of the noise distributions in order to verify stationary and Gaussian assumptions and obtain reasonable estimates for bias compensation.

The standard for AIS-BSs provides for a sentence containing information associated to the ToA of received messages, expanding the set of messages defined in the National Marine Electronics Association (NMEA) standard [20]. The specific field in the sentence allows representing a

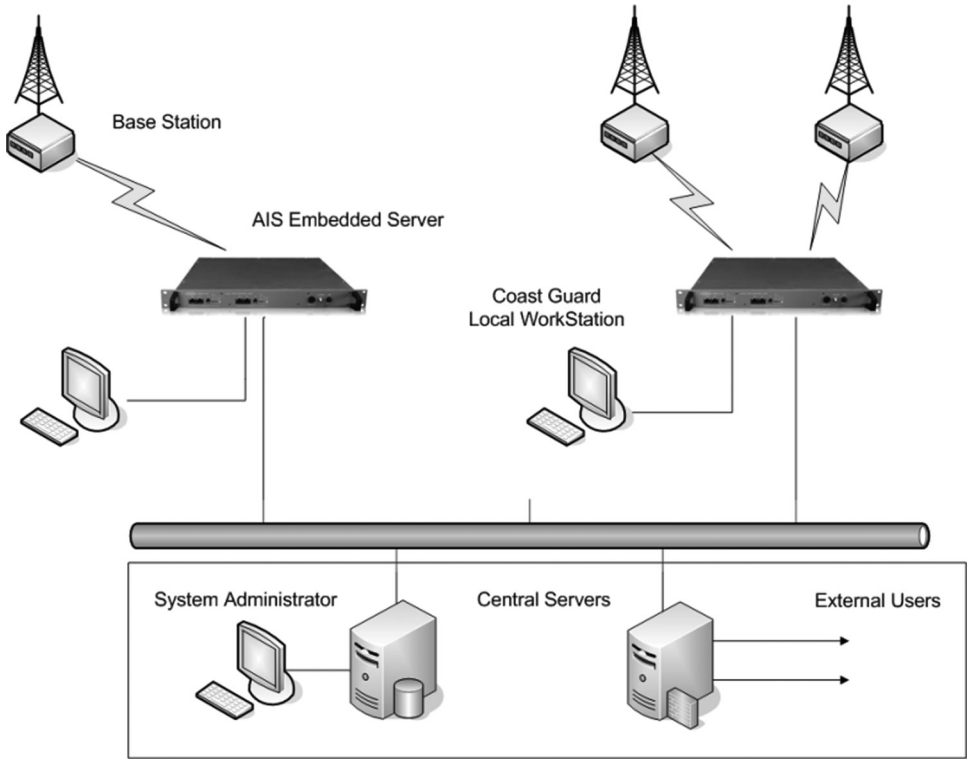


**Fig. 2** *Italian AIS network architecture*

precision up to 1 ns; however, a precision of 1 μs is currently obtained for the Italian Coast Guard National AIS network. Such precision is sufficient to estimate the location of the emission using MLAT and triangulation techniques as further discussed in this paper. The ToA is estimated by detecting the position of a specific marker in the AIS message, the start flag, relative to the slot start. The measurement is impacted by the timing error of the receiving station and by the quality of received signal. Low signal-to-noise ratio (SNR) may affect the accuracy of symbol clock recovery performed by the GMSK demodulator, which is currently limited by a resolution of 10.4 μs set by the internal sampling rate. Eventually, the accuracy of ToA may be greatly enhanced by BSs specifically designed to address this issue.

The ToF of the electromagnetic wave carrying the AIS message can be calculated as the difference between the ToA and the beginning of the time slot ($T_{\text{slot}}$) during which the message has been transmitted, that is

$$\text{ToF} = \text{ToA} - T_{\text{slot}} - \eta_{\text{tx}} - \eta_{\text{rx}} \tag{1}$$

where $\eta_{\text{tx}}$ and $\eta_{\text{rx}}$ are the transmitter and receiver timing errors, respectively. When it is possible to fully characterise the errors $\eta_{\text{tx}}$ and $\eta_{\text{rx}}$, an unbiased estimate of the ToF could be obtained and used to derive distance $R$ from the considered vessel and the receiving AIS base station (AIS-BS), that is, $R = c$ ToF where $c$ is the speed of light. Multiple distances from different AIS-BSs could then be used to find an unbiased estimate of the instantaneous vessel position using ToA-based triangulation.

Unfortunately the transmitter timing error $\eta_{\text{tx}}$ is generally unknown and, as mentioned before, can be in the order of tens of microseconds leading to large ranging uncertainties. Moreover, $\eta_{\text{tx}}$ is vessel-dependent because of differences in the electronics of different transmission equipment. This means that a full characterisation of $\eta_{\text{tx}}$ is not possible and the ToA measurements cannot be robustly used to directly solve the vessel localisation problem. The simplest idea in this case is to compare the received ToAs pairwise and use the TDoAs. Hence, assume the vessel under surveillance is within the coverage area of $n$ AIS-BSs, and then it is possible to collect $K = \binom{n}{2}$ TDoA$s$, that is

$$\begin{aligned} \tilde{\text{ToA}}_i &= \text{ToA}_i + \eta_{\text{tx}} + \eta_{\text{rx}_i} \\ \tilde{\text{ToA}}_j &= \text{ToA}_j + \eta_{\text{tx}} + \eta_{\text{rx}_j} \\ \text{TDoA}_{i,j} &= \text{ToA}_i - \text{ToA}_j + \eta_{\text{rx}_i} - \eta_{\text{rx}_j}, \\ & 1 \le j < i \le n \end{aligned} \tag{2}$$

where $\eta_{\text{rx}_i} \tilde{N}(\mu_i, \sigma_i^2)$ and $\eta_{\text{rx}_j} \tilde{N}(\mu_j, \sigma_j^2)$ are the receiver timing errors for the $i$th and $j$th AIS-BS, respectively. We can then rewrite the **TDoA**s vector as follows

$$\mathbf{TDoA} = \begin{bmatrix} \text{TDoA}_{2,1} \\ \vdots \\ \text{TDoA}_{n,1} \\ \text{TDoA}_{3,2} \\ \vdots \\ \text{TDoA}_{n,n-1} \end{bmatrix} + v,\ v \tilde{N}(\mu_{\text{TDoA}}, R_{\text{TDoA}}) \tag{3}$$

$$\boldsymbol{\mu}_{\mathbf{TDoA}} = \begin{bmatrix} \mu_2 - \mu_1 & \dots & \mu_3 - \mu_2 & \dots & \mu_n - \mu_{n-1} \end{bmatrix} \tag{4}$$

$$\boldsymbol{R}_{\mathbf{TDoA}} = \text{blockdiag}\left(R_1,\ R_2,\ \dots,\ R_K\right) \tag{5}$$

$$\boldsymbol{R_1} = \begin{bmatrix} \sigma_1^2 + \sigma_2^2 & \cdots & \sigma_1^2 \\ \vdots & \ddots & \vdots \\ \sigma_1^2 & \cdots & \sigma_1^2 + \sigma_n^2 \end{bmatrix} \tag{6}$$

$$\boldsymbol{R_2} = \begin{bmatrix} \sigma_2^2 + \sigma_3^2 & \cdots & \sigma_2^2 \\ \vdots & \ddots & \vdots \\ \sigma_2^2 & \cdots & \sigma_2^2 + \sigma_n^2 \end{bmatrix} \tag{7}$$

$$R_K = \sigma_n^2 + \sigma_{n-1}^2 \tag{8}$$

As for the parameters ($\mu_i$, $\sigma_i$), some a priori knowledge might be available from the receivers' characteristics. Since this is not our case, an estimate of ($\mu_{\text{TDoA}}$, $R_{\text{TDoA}}$) can be obtained using batch data or over a moving time-window. In addition, if ToA measurements are optimally obtained using correlation processing, the standard deviations $\sigma_i$ can be modelled using the Cramer–Rao lower bound [21]

$$\sigma_i \ge \frac{c}{B \cdot \sqrt{\text{SNR}_i}} \tag{9}$$

where $B$ is the signal bandwidth and $\text{SNR}_i$ is the SNR of the $i$th channel. $\text{SNR}_i$ could be modelled by means of Friis transmission equation as $\hat{\text{SNR}}_i = \text{SNR}_i(\hat{x}_k)$, where $\hat{x}_k$ is the estimated vessel position at time $k$.

A noise analysis was performed using real AIS data collected for ~9 h over 3 days. Results are depicted in Fig. 3 for a subset of the Italian AIS network. Both AIS service messages (i.e. BS reports periodically transmitted [10]) and AIS messages from verified vessel trajectories were used to estimate the noise distribution.

From the results in Fig. 3, it is immediate to verify the assumed Gaussian properties and extract reasonable estimates for each bias $\mu_i - \mu_j$ and variance $\sigma_i^2 + \sigma_j^2$. Finally, since the bias $\mu_{\text{TDoA}}$ appears to be sufficiently stationary, we can use the estimate $\hat{\mu}_{\text{TDoA}}$ for bias compensation.

## 4 TDOA-based vessel localisation

The problem of estimating an emitter position from TDoA measurements occurs in a wide range of applications. Conceptually, a correlation analysis of the received signal from two receivers should give rise to one hyperbolic function. However, because of TDoA measurement uncertainty, it is not possible to use multiple hyperbolas to robustly determine a unique intersection [16]. We in fact face a non-linear estimation problem defined as follows. Assume that a vessel transmitting AIS messages are located at position $P_v = (x_v, y_v)$. Let $P = (x, y)$ be a generic point in geodetic coordinates and let $P_i^{\text{RX}} = \left(x_i^{\text{RX}}, y_i^{\text{RX}}\right)$ be the position vector for the $i$th AIS-BS. Then a non-linear estimate of $P_v$ is found as

$$\hat{P}_v = \arg\min_P \sum_{i>j} d\left(\text{TDoA}_{i,j},\ h\left(P,\ P_i^{\text{RX}},\ P_j^{\text{RX}}\right)\right) \tag{10}$$




doi: 10.1049/iet-rsn.2014.0292

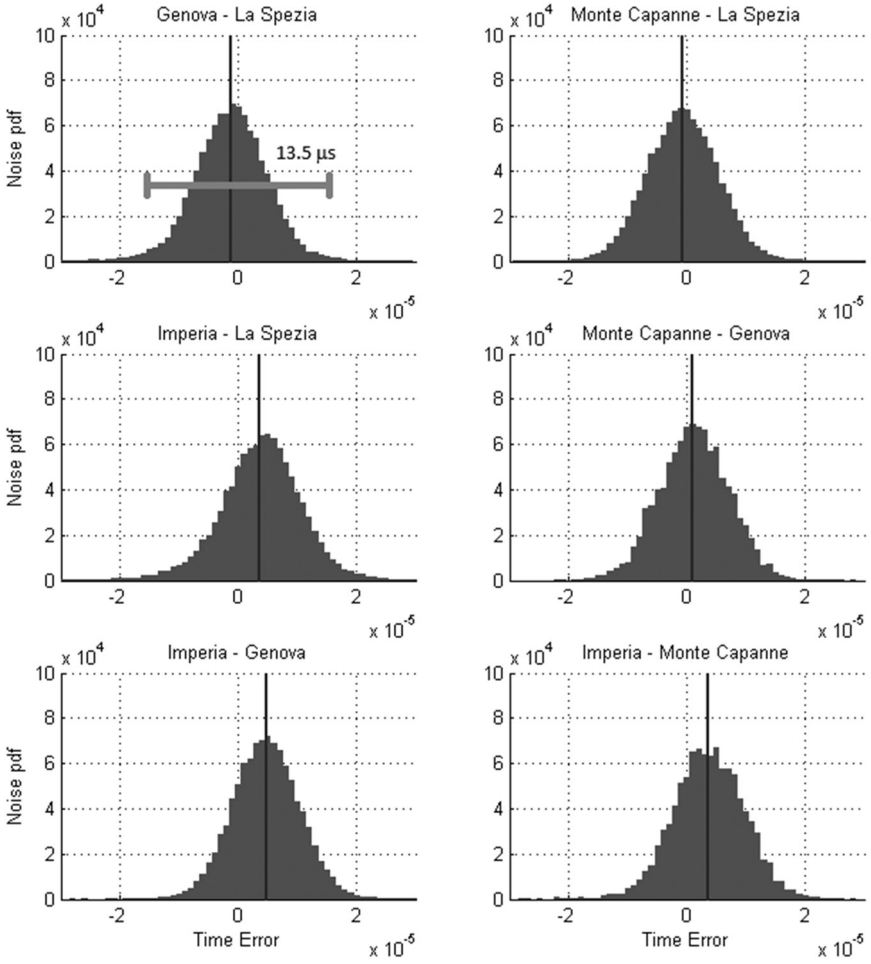


**Fig. 3** *PDF of the TDoA errors for a set of receiving station pairs. Relevant bias $\mu_i - \mu_j$ (vertical lines) can be readily estimated. Note also that an upper bound of ±13.5 μs can be selected so that about 95% of noise PDF is included.*

where

$$h\left(P,\ P_i^{\mathrm{RX}},\ P_j^{\mathrm{RX}}\right) = \left(\sqrt{\left(x - x_i^{\mathrm{RX}}\right)^2 + \left(y - y_i^{\mathrm{RX}}\right)^2}. - \sqrt{\left(x - x_j^{\mathrm{RX}}\right)^2 + \left(y - y_j^{\mathrm{RX}}\right)^2}\right) \Big/ c \quad (11)$$

and $d(\cdot)$ is a suitable distance. This could be for instance the square of the Euclidean distance (i.e. least-squares estimate) or the Mahalanobis distance (i.e. maximum-likelihood estimate).

Since we are instead interested in finding the associated estimation error, we can use the following approach. Consider for instance a fixed grid of points $P$ in geodetic coordinates, and set an upper bound on the differential time uncertainty as $K = 13.5$ μs, which corresponds to about 4 km location uncertainty. This bound was chosen so that 95% of the noise 'probability density function' (PDF) is covered (see Fig. 3). Then we can easily identify the set of points $P$ that satisfy the following set of inequalities, that is

$$\left|h\left(P,\ P_i^{\mathrm{RX}},\ P_j^{\mathrm{RX}}\right) - \mathrm{TDoA}_{i,j}\right| \leq c \cdot K, \quad 1 \leq j < i \leq n \quad (12)$$

The locus of points where (12) is verified is a hyperbola with uncertainty in the flat-earth approximation case [16]. The area contained by all intersections can be thought of as a measure of the estimation error. Examples of this are shown in Figs. 4 and 5 where the AIS message emission is located within the intersection of the hyperbolic functions as derived from the TDoA measurements between three and four stations, respectively.

Then assuming a Gaussian distribution for the noise terms (as verified in the previous section), the associated estimation covariance is given by the minimum volume ellipse enclosing all points that verified (12).

A more rigorous approach uses the Mahalanobis distance

$$d_{i,j}^M = h\left(P,\ P_i^{\mathrm{RX}},\ P_j^{\mathrm{RX}}\right) - \mathrm{TDoA}_{i,j}$$
$$\boldsymbol{\Delta}_M = \left[\begin{array}{ccc} d_{2,1}^M & \cdots & d_{n,n-1}^M \end{array}\right] \quad (13)$$
$$\hat{\boldsymbol{P}}_v = \arg\min_P \boldsymbol{\Delta}_M \hat{\boldsymbol{R}}_{\mathrm{TDoA}}^{-1} \boldsymbol{\Delta}_M^{\mathrm{T}}$$

where $\hat{\boldsymbol{P}}_v$ is the maximum-likelihood estimate and $\hat{\boldsymbol{R}}_{\mathrm{TDoA}}$ is an estimate of the TDoA covariance given in (6). In this case, the error area is given by the set of points that verify the following Chi-Square test

$$\boldsymbol{\Delta}_M \hat{\boldsymbol{R}}_{\mathrm{TDoA}}^{-1} \boldsymbol{\Delta}_M^{\mathrm{T}} \leq \gamma(\alpha,\ K) \quad (14)$$

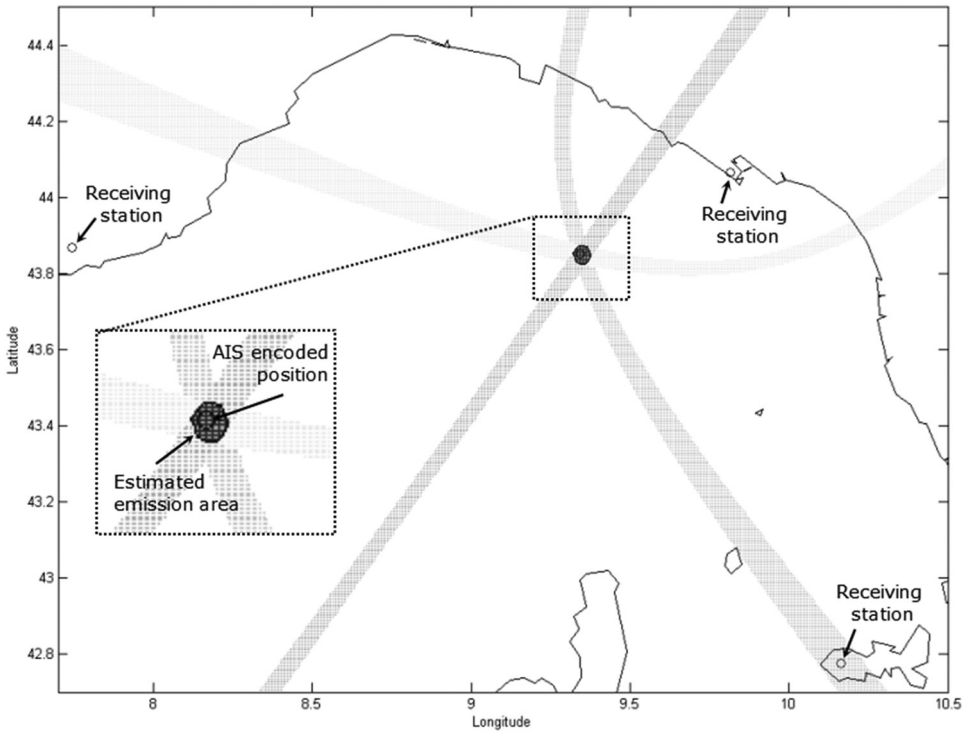


**Fig. 4** *Radiolocation of the AIS emission in the Ligurian Sea as the intersection of the TDoAs hyperbolic functions between three receiving stations. AIS encoded position falls within the estimated emission area.*

where $\gamma(\alpha, K)$ is the value of the Chi-Square distribution for $K$ degrees of freedom and $1-\alpha$ confidence. Note that for both problems in (10) and (13), we are assuming either zero TDoA bias, that is, $\boldsymbol{\mu}_{\mathrm{TDoA}} = 0_{Kx1}$ or that a reasonable estimate $\hat{\boldsymbol{\mu}}_{\mathrm{TDoA}}$ is available for bias compensation. This is possible in our case since the time error bias at the receiver is sufficiently stationary in time and space (Section 3). The output of the TDoA-based localisation procedure is a pair $(\mathbf{z}_k, \boldsymbol{R}_k)$. Specifically, $z_k$ containing the vessel location estimate in geodetic coordinates and $\boldsymbol{R}_k$ is a covariance matrix describing the minimum volume ellipse enclosing the set of points that verify (14). Time integration is then

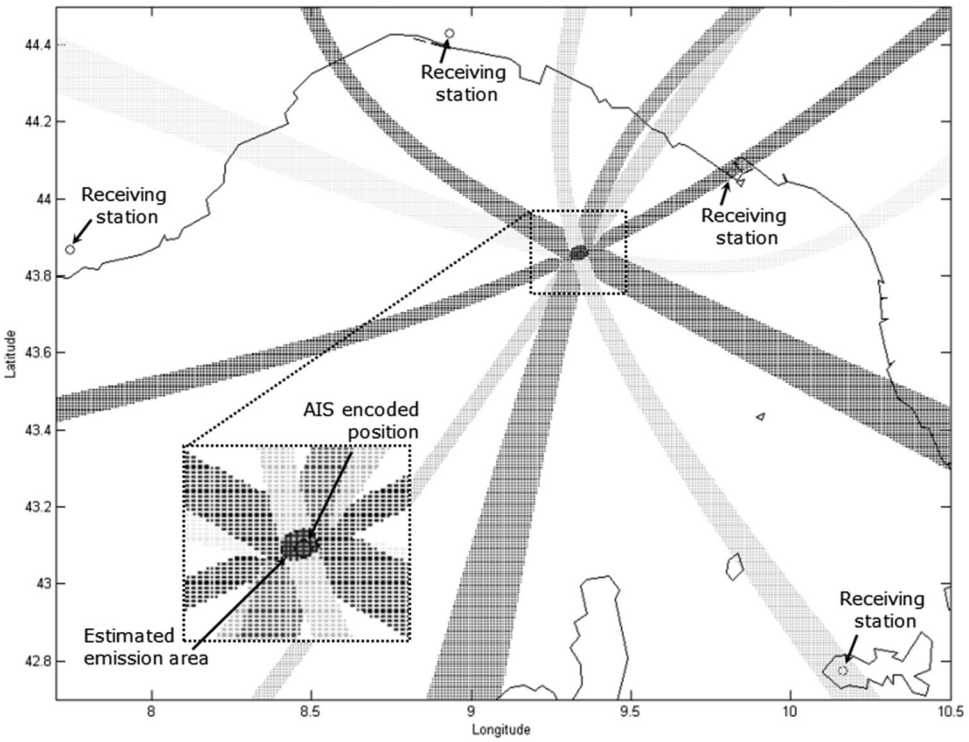


**Fig. 5** *AIS emission is received by four stations. Additional AIS-BS yields a reduction of the intersection area between the available TDoAs, thus reducing the localisation uncertainty.*




doi: 10.1049/iet-rsn.2014.0292

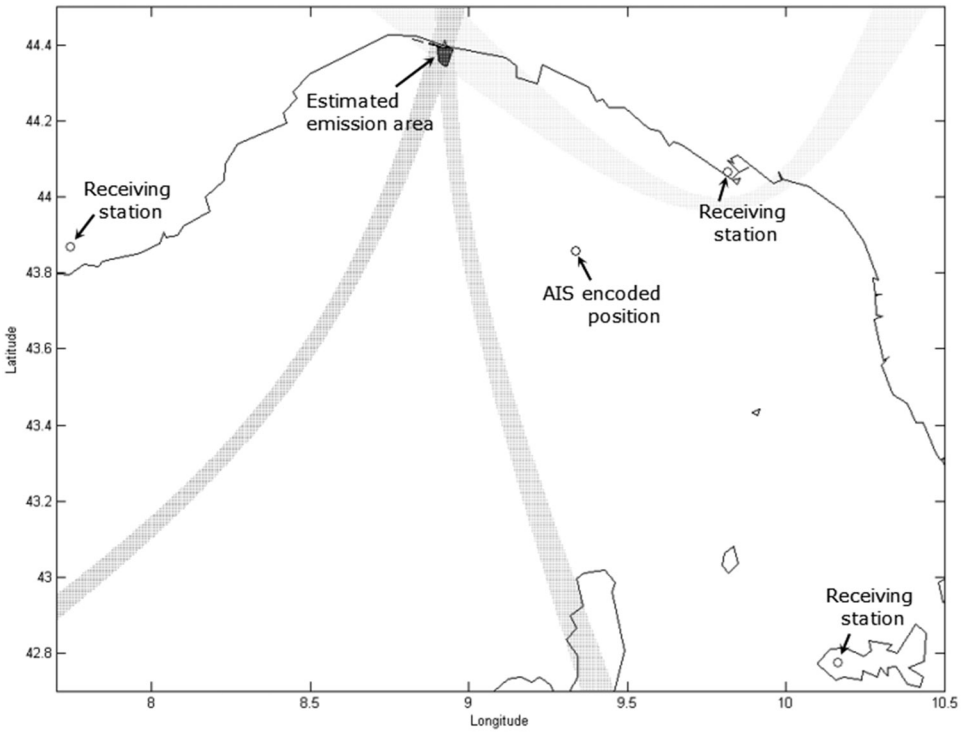


**Fig. 6** *Radiolocation results highlight that the message originally transmitted in open seas is repeated by the BS in Genoa*

performed by using ($z_k$, $\boldsymbol{R}_k$) as inputs of a suitable EKF as described in the following section.

Another localisation example is reported in Fig. 6. Here the AIS-based radiolocation and the declared vessel position are sensibly different: this happens when the AIS message from the vessel in open seas is repeated by a BS (in accordance with AIS standard, a BS can be requested to store and forward a position message sent by a vessel), easily located in Genoa in this case.

The spatial distribution of BSs is central to the performance of the radiolocation process. This is given by the extent of the uncertainty at a specific location in space and varies depending on the transmitter position with respect to the receiving stations. For instance, in Fig. 7 the message is received by three stations and the emission location can be verified. However, the error area is quite large. This happens because the vessel is far away from all the sensors baselines and the angles of arrivals are similar. To better clarify this point we performed a geometric analysis of the localisation precision with reference to the positions of the Italian BSs. Results are given in Fig. 8, where we show how the estimated precision varies in space for different AIS network configurations.

## 5 Vessel tracking using an EKF

As previously mentioned, at time step $k$ the MLAT procedure gives as output a pair ($\boldsymbol{z}_k$, $\boldsymbol{R}_k$) for each vessel, where $\boldsymbol{z}_k$ is the estimated vessel position and $\boldsymbol{R}_k$ its associated error covariance. We can then perform model-based time integration by recursively solving the Chapman–Kolmogorov integral and Bayes equation [22]. In fact, Bayesian methods provide a rigorous framework for dynamic state estimation problems. The idea is to construct the PDF of the system state based on all the available information, and then find an approximation of such a posteriori PDF. Classical inference methods for 'non-linear filtering' are the EKF [23], based on linearisation of the system about the current state estimate, and the unscented Kalman filter [24], based on a deterministic sampling of the a posteriori PDF. Improved tracking accuracy can be generally achieved by means of sequential Monte Carlo (SMC) methods like the particle filter (PF) [25].

For our specific problem, we can use a non-linear equation to efficiently describe the vessel trajectory. In fact, let $x_k$, $y_k$, $v_k$ and $c_k$ be the latitude, longitude, SOG and COG at time $k$. Then the geodetic vessel position at time $k+1$ is given by

$$x_{k+1} = \frac{180}{\pi}\left(\sin\left(x_k\frac{\pi}{180}\right)\cos\left(v_k\frac{T_k}{R_{\text{earth}}}\right) + \cos\left(x_k\frac{\pi}{180}\right)\sin\left(v_k\frac{T_k}{R_{\text{earth}}}\right)\cos(c_k)\right) \tag{15}$$

(see (16) at the bottom of the page)

where $R_{\text{earth}}$ is the Earth radius and $T_k$ is the sampling interval of the filtering problem, that is, the time interval between two consecutive (lat, lon) estimates from the MLAT procedure. As for the SOG $v_k$ and COG $c_k$, we assume zero-dynamic with Gaussian noise. Then by choosing $\boldsymbol{x}_k = [x_k\ y_k\ v_k\ c_k]^{\text{T}}$ as the system state, we can

$$y_{k+1} = y_k + \frac{180}{\pi}\arctan\left(\frac{\cos\left(x_k(\pi/180)\right)\sin\left(v_k(T_k/R_{\text{earth}})\right)\sin(c_k)}{\cos\left(v_k(T_k/R_{\text{earth}})\right) - \sin\left(x_k(\pi/180)\right)\sin\left(x_{k+1}(\pi/180)\right)}\right) \tag{16}$$

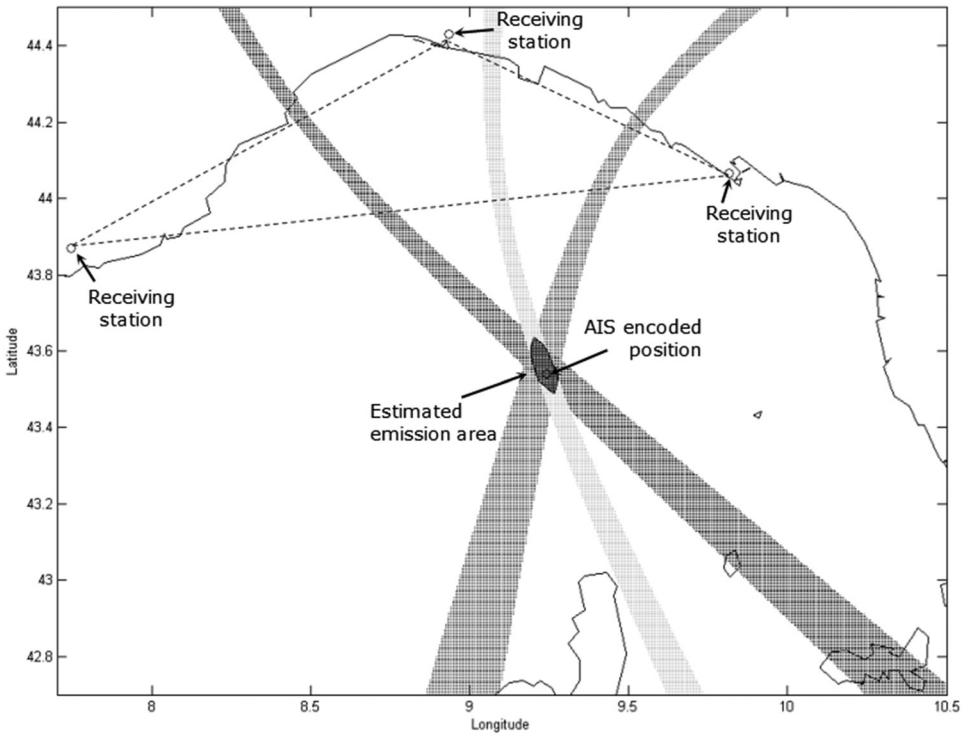


**Fig. 7** *Radiolocation uncertainty changes depending on the position of the emission and the receivers' location*

describe our problem using the following dynamic system with non-linear dynamics and linear measurement equation, that is

$$\boldsymbol{x}_{k+1} = f(\boldsymbol{x}_k) + \boldsymbol{w}_k \tag{17}$$

$$\boldsymbol{z}_k = \boldsymbol{H}_k \boldsymbol{x}_k + \boldsymbol{v}_k \tag{18}$$

$$\boldsymbol{H}_k = \begin{bmatrix} 1 & 0 & 0 & 0 \\ 0 & 1 & 0 & 0 \end{bmatrix} \tag{19}$$

where $\boldsymbol{w}_k \sim N(0, Q_k)$ and $\boldsymbol{v}_k \sim N(0, R_k)$ are zero-mean white Gaussians representing the process and measurement noise, respectively. Given the initial state estimate $\boldsymbol{x}_0$ and associated error covariance $\boldsymbol{P}_0$, the EKF for the system in (15)–(18) is given by the following two step recursion: Prediction step

$$\hat{\boldsymbol{x}}_{k|k-1} = f(\hat{\boldsymbol{x}}_{k-1|k-1}) \tag{20}$$

$$\boldsymbol{P}_{k|k-1} = \boldsymbol{F}_{k-1} \boldsymbol{P}_{k-1|k-1} \boldsymbol{F}_{k-1}^{\mathrm{T}} + \boldsymbol{Q}_k \tag{21}$$

$$\boldsymbol{F}_{k-1} = \left. \frac{\partial f}{\partial \boldsymbol{x}_{k-1}} \right|_{\hat{\boldsymbol{x}}_{k-1|k-1}} \tag{22}$$

Update step

$$\boldsymbol{S}_k = \boldsymbol{H}_k \boldsymbol{P}_{k|k-1} \boldsymbol{H}_k^{\mathrm{T}} + \boldsymbol{R}_k \tag{23}$$

$$\boldsymbol{K}_k = \boldsymbol{P}_{k|k-1} \boldsymbol{H}_k^{\mathrm{T}} \boldsymbol{S}_k^{-1} \tag{24}$$

$$\hat{\boldsymbol{x}}_{k|k} = \hat{\boldsymbol{x}}_{k|k-1} + \boldsymbol{K}_k (\boldsymbol{z}_k - \boldsymbol{H}_k \hat{\boldsymbol{x}}_{k|k-1}) \tag{25}$$

$$\boldsymbol{P}_{k|k} = (\boldsymbol{I}_{n \times n} - \boldsymbol{K}_k \boldsymbol{H}_k) \boldsymbol{P}_{k|k-1} \tag{26}$$

where $F_{k-1}$ in (20) is the Jacobian of the non-linear time evolution $f(\cdot)$ and $(\hat{\boldsymbol{x}}_{k|k}, P_{k|k})$ are the state estimate and associated error covariance at time $k$.

## 6 Tracking results

We now report the tracking results obtained from processing real AIS data collected by the Italian terrestrial network for ~3 h. Results for a single vessel are depicted in Figs. 9–11. Specifically, in Fig. 9 we report the reference vessel trajectory from GNSS data, the (lat, lon) estimates from the localisation procedure and the EKF position estimates. Note that we report the reference vessel location only when the AIS message is received by at least three AIS-BSs. This is done in order to highlight the gaps of TDoA measurements because of non-perfect coverage. The estimation errors over time for the TDoA localisation and after EKF processing are depicted in Fig. 10. Finally, the EKF results in estimating the vessel kinematics, that is, SOG and COG, are depicted in Fig. 11.

We performed the same tracking analysis for all the vessel trajectories within the coverage of at least three AIS-BSs. Results for a vessel leaving the port of La Spezia are depicted in Figs. 12–14. Specifically, the (lat, lon) tracking results are depicted in Fig. 12, the estimation errors are reported in Fig. 13 and the EKF results in estimating the vessels COG and SOG are depicted in Fig. 14. Significant differences in terms of MLAT position error can be seen from Fig. 13 if compared with Fig. 10 for a vessel leaving the port of Savona. This is because of better coverage in the area of La Spezia, that is, there are four AIS-BSs available most of the time, as predicted by the static analysis reported in Fig. 8. The same metrics are depicted for a third vessel trajectory in Figs. 15–17. From the results, we can verify that the average location error of the EKF is always below 2 km, thus confirming the effectiveness of the radiolocation technique.




doi: 10.1049/iet-rsn.2014.0292

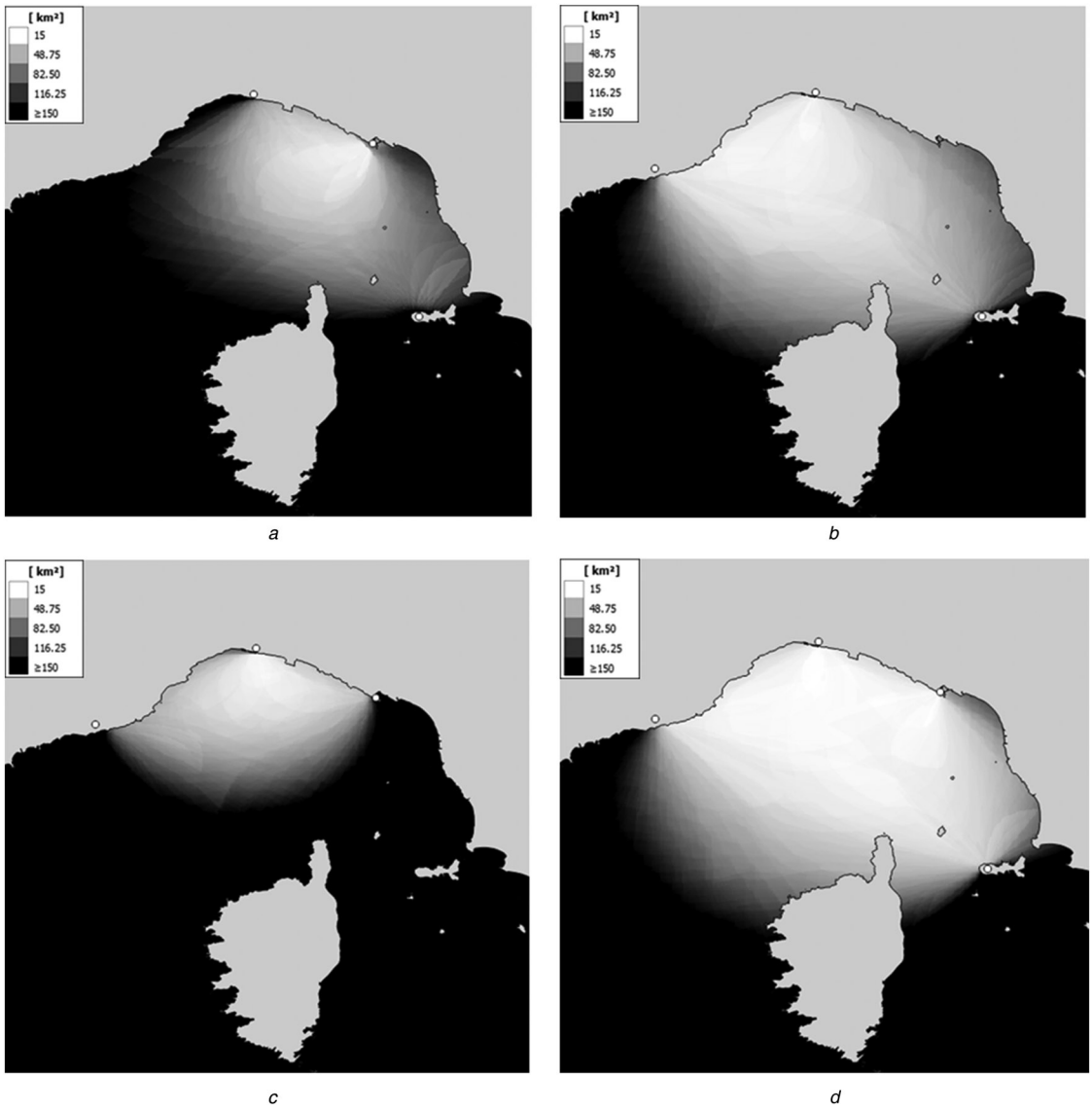


**Fig. 8** *Radiolocation uncertainty limits obtained when a single AIS message is received from different BSs using*

*a–c* Three TDoA measurements and considering K = 13.5 is for each TDoA
*d* Resulting performance when the message is received by four BSs, leading to six TDoAs

It is worth noting that the number of scans needed by the EKF to converge to the true COG and SOG values sensibly varies from track to track. This is because of a number of factors, chief among them the positions of the transmitter and the receivers, the motion and velocity of the vessel and the variable time between scans. The latter depends on (i) the

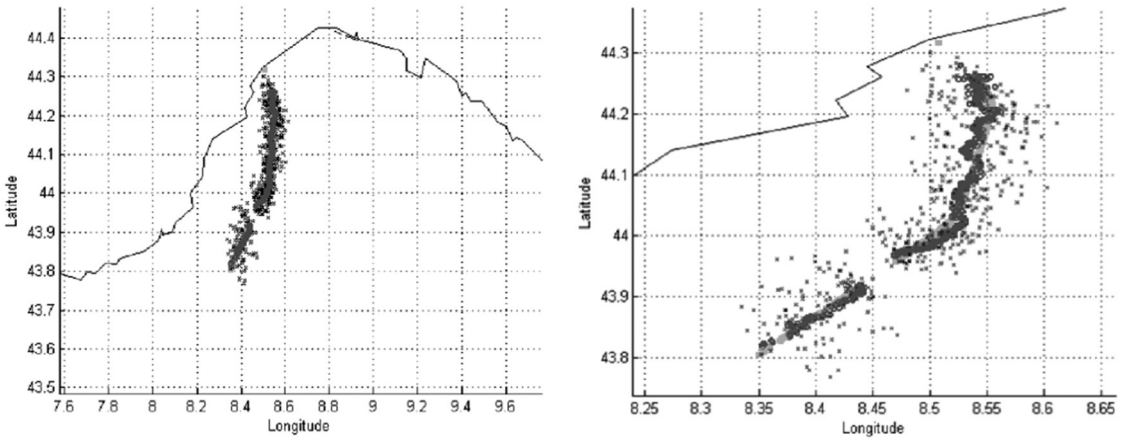


**Fig. 9** *Tracking results for a single vessel leaving the port of Savona (left) and zoomed trajectory. True trajectory (light grey), estimates from the MLAT procedure (black crosses) and EKF position estimates (dark grey).*

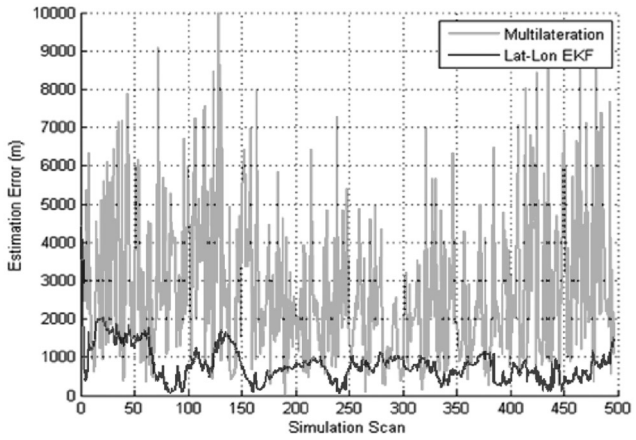


**Fig. 10** *Localisation error over time for a single vessel trajectory: MLAT procedure and EKF in geodetic coordinates.*

AIS transmission rate, which changes according to the vessel manoeuvre and velocity and (ii) the rate of reception of the message by three or more stations. Additional tuning of the filter parameters could lead to improved performance in terms of the estimated COG and SOG. In general, reducing the filter process noise leads to more precise estimates for the vessel kinematics. This however might reduce the filter robustness and precision in terms of location estimates.

Finally, collective results are depicted in Fig. 18 where we report the tracking results for all considered vessel trajectories in the north Tyrrhenian. Specifically, the estimates from the multilateration procedure (black crosses) and the EKF position estimates (dark grey) almost completely cover the true vessel trajectories (light grey). As previously mentioned, we consider only the vessel trajectories within the coverage area of at least three AIS-BS.

Two final remarks on the results in Fig. 18: (i) some of the estimates from the MLAT procedure are on land; this is due to the fact that the MLAT procedure is performed without applying land constraints to avoid biasing the EKF measurements. However, Bayes optimal methods to enforce such constraints exist [26] and will be used in future developments. (ii) Some of the initial/final estimates from the MLAT procedure are far away from the true vessel location (area highlighted by the circle): this happens when there is a non-optimal spatial distribution of the AIS-BSs, leading to multiple solutions (ghost estimates) to the TDoA localisation problem. This problem could be solved by extending the overlapping coverage of the AIS network and/or by using a SMC filter, for example, the PF, to keep track of the intrinsically multimodal posterior PDF. We will in fact consider the use of particle filtering for future research since it should lead to more robust results for decision making.

The demonstrated average performance of the proposed radiolocation and tracking technique based on EKF confirm

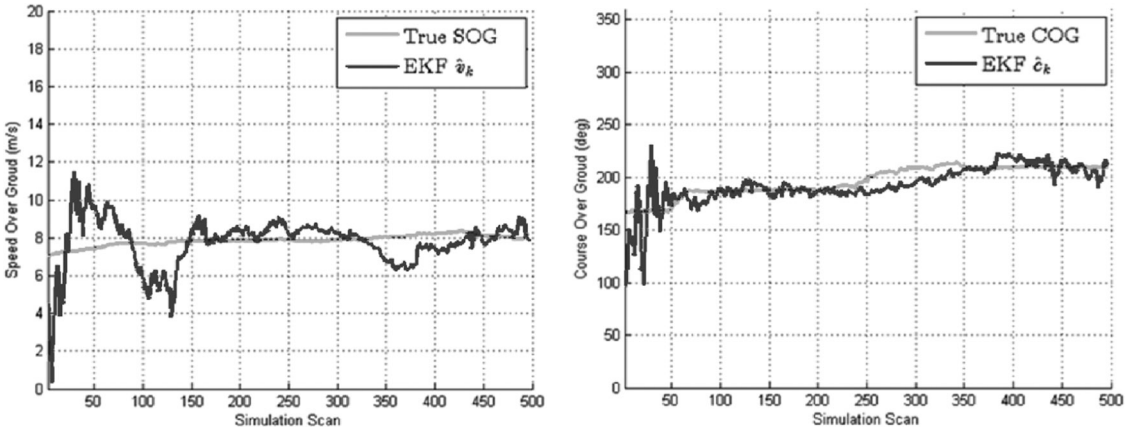


**Fig. 11** *EKF results in estimating the vessel kinematics. True and estimated SOG (left); true and estimated COG (right).*

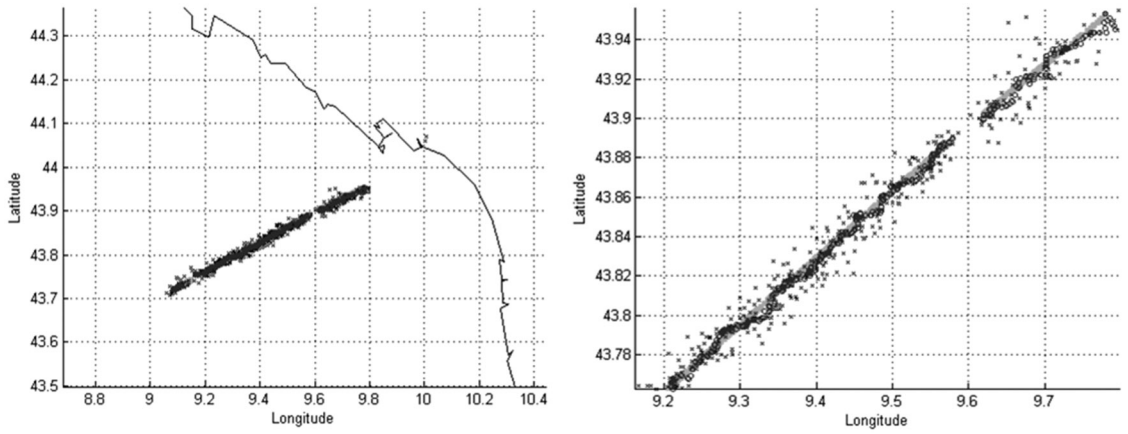


**Fig. 12** *Tracking results for a single vessel leaving the port of La Spezia (left) and zoomed trajectory. True trajectory (light grey), estimates from the MLAT procedure (black crosses) and EKF position estimates (dark grey).*




doi: 10.1049/iet-rsn.2014.0292

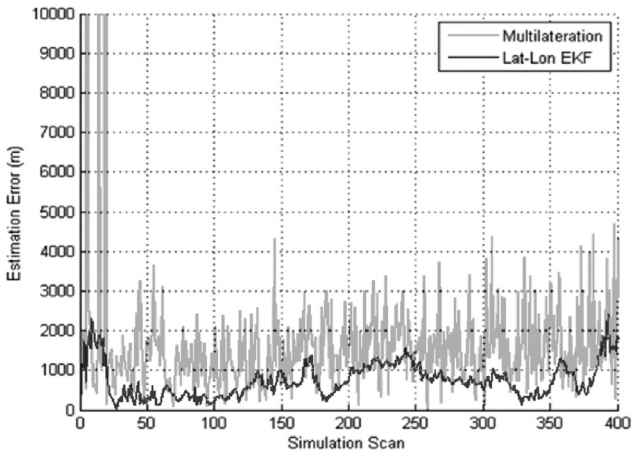


**Fig. 13** *Localisation error over time for a single vessel trajectory: MLAT procedure and EKF in geodetic coordinates.*

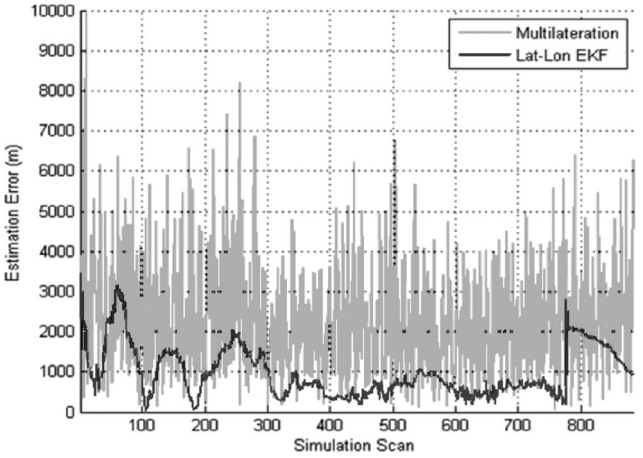


**Fig. 16** *Localisation error over time for a single vessel trajectory: MLAT procedure and EKF in geodetic coordinates.*

that the approach could be used to perform automatic validation of declared GNSS positions encoded in the broadcast AIS messages. This could be performed using a single-step gate validation [27] or a more effective binary hypothesis testing over a moving time-window [28]. The former approach may be sufficient if the EKF estimate is close to the true vessel position but is intrinsically prone to a large number of false positives. A more effective way of performing data validation is the use of a binary hypothesis test where $H_1$ is the hypothesis for no anomaly and $H_0$ is the hypothesis for ongoing anomaly. Given the random variable $Z$ representing the MLAT output and $z$ its

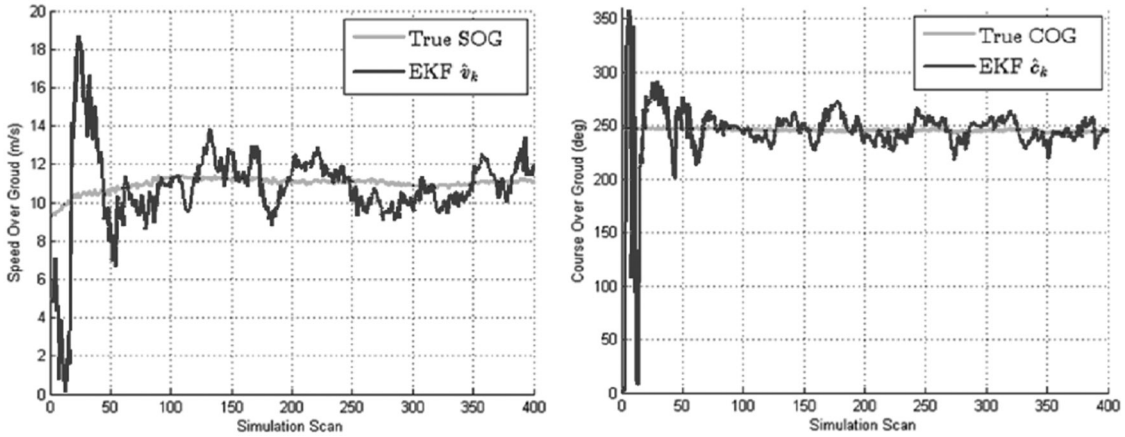


**Fig. 14** *EKF results in estimating the vessel kinematics. True and estimated SOG (left); true and estimated COG (right).*

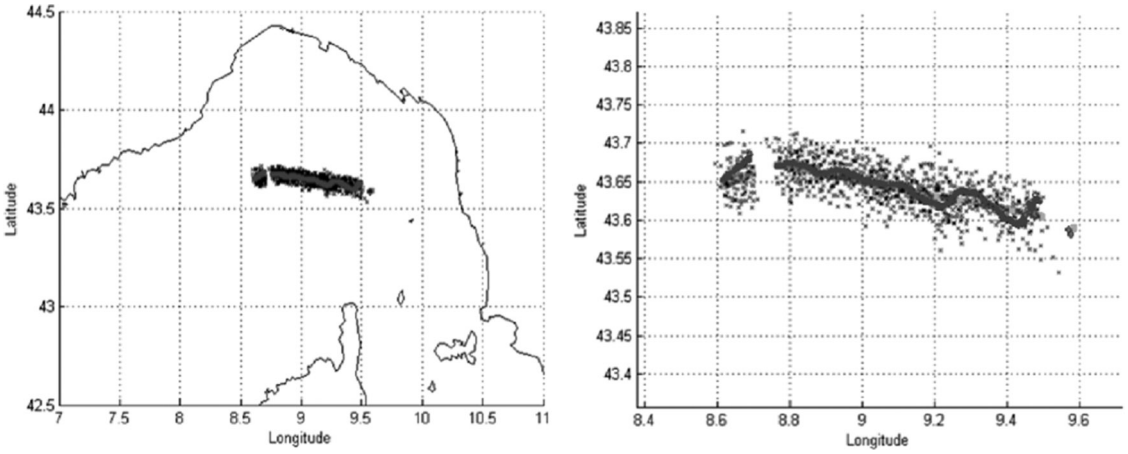


**Fig. 15** *Tracking results for a single vessel travelling westbound. True trajectory (light grey), estimates from the MLAT procedure (black crosses) and EKF position estimates (dark grey).*

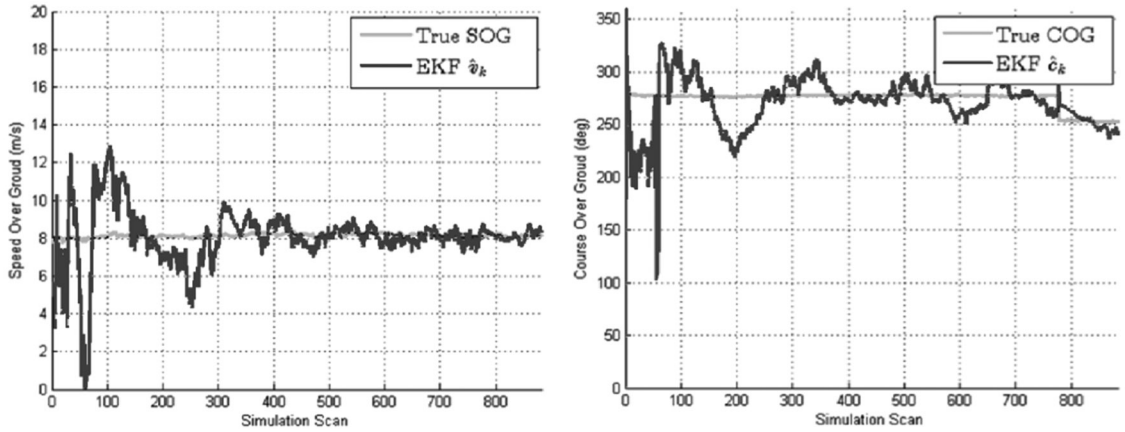


**Fig. 17** *EKF results in estimating the vessel kinematics. True and estimated SOG (left); true and estimated COG (right).*

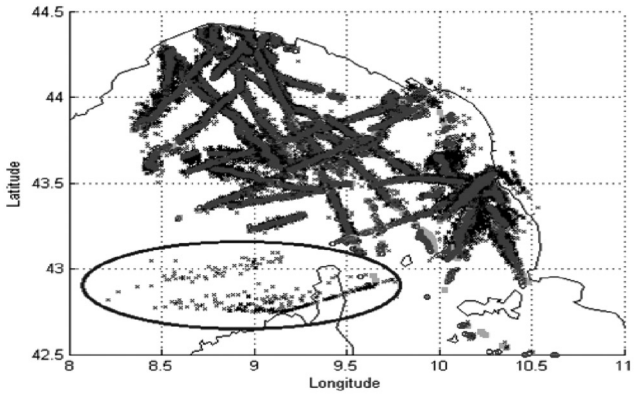


**Fig. 18** *Tracking results for a set of trajectories using real AIS data collected by the Italian terrestrial network over about 3 h and received by three or more stations. It is worth noting that AIS tracks received by < 3 stations are not plotted.*

realisation, the binary hypothesis test is performed by comparing the likelihood ratio $p_{z|H_1}(Z|H_1)/p_{z|H_0}(Z|H_0)$ against a decision threshold defined by the prior and Bayes risk [28]. In particular, $p_{z|H_1}(Z|H_1)$ represents the likelihood of observing $z$ given the vessel is located in the GNSS declared position and $p_{z|H_0}(Z|H_0)$ is the likelihood of observing $z$ given the vessel is following the EKF estimated track. Both the single-step validation gate and the binary hypothesis test should be applied only when the MLAT confidence is high (see Fig. 8) in order to minimise the anomaly false alarm rate. These aspects will be the subject of future research activities.

## 7 Conclusions

A number of activities (traffic monitoring and management, Search and Rescue etc.) at sea are based on information provided by vessels through AIS. AIS communication system is prone to tampering and spoofing, thus the validation of the data provided through a reporting system such as AIS is an important issue faced by authorities involved in the different areas of maritime surveillance. It is not known the level of actual alteration of AIS provided data which, nevertheless, is expected to increase in the future. Therefore it is important to improve the assessment of the reliability of the position data transmitted by ships in an automated way to increase the safety of the seas. This paper has successfully addressed this issue offering an effective method to validate the position data sent by the ships through AIS, with an accuracy that ranges from few hundreds of metres, in optimal condition, to few kilometres in marginal situation. It has to be noted that from the operational point of view such accuracy can be considered more than acceptable. The proposed method collects the data provided by the network of stations receiving the AIS messages transmitted by the ship at seas and uses the time stamp (ToA) added by the AIS-BSs to the messages received from the ship. The algorithm allows, in few steps, to narrow down the estimated position of the ship to few hundreds of metres (without using in any way the position reported by the ship). The algorithm described in this paper has been successfully tested using real, anonymised data provided by the Italian Coast Guard, demonstrating that EKF outperforms MLAT for maritime situational awareness. Moreover, the tracks originated by the proposed methodology can be thought of as the input of automatic tools for the detection of anomalies related to AIS data verification, which represent the next stage of this research activity.

## 8 Acknowledgments

The authors would like to thank the reviewers for their valuable contribution in improving this paper.

## 9 References

1 Angrisano, A., Gaglione, S., Gioia, C.: 'Performance assessment of aided global navigation satellite system for land navigation', *IET Radar Sonar Navig.*, 2013, **7**, (6), pp. 671–680
2 Safety of Life at Sea (SOLAS) convention Chapter V, Regulation 19
3 Directive 2002/59/EC of the European Parliament and of the Council establishing a Community vessel traffic monitoring and information system, as amended by Directive 2009/17/EC and Commission Directive 2011/15/EU
4 Baldauf, M., Benedict, K., Motz, F.: 'Aspects of technical reliability of navigation systems and human element in case of collision avoidance'. Proc. Navigation Conf. & Exhibition, 2008
5 Høye, G.K., Eriksen, T., Meland, B.J., Narheim, B.T.: 'Space-based AIS for global maritime traffic monitoring', *Acta Astronaut.*, 2008, **62**, (2), pp. 240–245
6 Pallotta, G., Vespe, M., Bryan, K.: 'Vessel pattern knowledge discovery from AIS data: a framework for anomaly detection and route prediction', *Entropy*, 2013, **15**, (6), pp. 2218–2245
7 Ristic, B., La Scala, B., Morelande, M., Gordon, N.: 'Statistical analysis of motion patterns in AIS data: anomaly detection and motion prediction'. Proc. 11th IEEE Int. Conf. on Information Fusion, 2008




doi: 10.1049/iet-rsn.2014.0292

8 Roy, J.: 'Anomaly detection in the maritime domain'. SPIE Defense and Security Symp., Int. Society for Optics and Photonics, 2008
9 Kroener, U., Dimc, F.: 'Hardening of civilian GNSS trackers'. Proc. of the Third GNSS Vulnerabilities and Solutions Conf., 2010
10 'Ship Tracking Hack Makes Tankers Vanish from View'. Available at http://www.technologyreview.com/news/520421/ship-tracking-hack-makes-tankers-vanish-from-view, accessed July 2006
11 Guerriero, M., Willett, P., Coraluppi, S., Carthel, C.: 'Radar/AIS data fusion and SAR tasking for maritime surveillance'. Proc. 11th IEEE Int. Conf. on Information Fusion, 2008
12 Katsilieris, F., Braca, P., Coraluppi, S.: 'Detection of malicious AIS position spoofing by exploiting radar information'. Proc. 16th IEEE Int. Conf. on Information Fusion, 2013, pp. 1196–1203
13 Vespe, M., Sciotti, M., Burro, F., Battistello, G., Sorge, S.: 'Maritime multi-sensor data association based on geographic and navigational knowledge'. Proc. IEEE Radar Conf., 2008
14 TRITON (TRusted vessel Information from Trusted On-board iNstrumentation) project, funded by the EU within the Seventh Framework Programme (FP7)
15 Chan, Y.T., Ho, K.C.: 'A simple and efficient estimator for hyperbolic location', *IEEE Trans. Signal Process.*, 1994, **42**, (8), pp. 1905–1915
16 Gustafsson, F., Gunnarsson, F.: 'Positioning using time-difference of arrival measurements'. Proc. IEEE Int. Conf. on Acoustics, Speech, and Signal Processing, 2003, vol. 6, p. VI-553
17 Pourvoyeur, K., Mathias, A., Heidger, R.: 'Investigation of measurement characteristics of MLAT/WAM and ADS-B'. Proc. IEEE Tyrrhenian Int. Workshop on Digital Communications-Enhanced Surveillance of Aircraft and Vehicles, 2011, pp. 203–206
18 Galati, G., Gasbarra, M., Magaro, P., De Marco, P., Mene, L., Pici, M.: 'New approaches to multilateration processing: analysis and field evaluation'. Proc. Third IEEE European Radar Conf., 2006, pp. 116–119
19 Recommendation ITU-R M 1371–4: 'Technical characteristics for a universal shipborne automatic identification system using time division multiple access in the VHF maritime mobile band'
20 IEC 62320–1: Maritime navigation and radio communication equipment and systems – Automatic Identification System (AIS) – Part 1: AIS Base Stations – Minimum operational and performance requirements, methods of testing and required test results
21 Kay, S.M.: 'Fundamentals of statistical signal processing: estimation theory' (Prentice-Hall Inc., Upper Saddle River, NJ, USA, 1993)
22 Anderson, B.D., Moore, J.B.: 'Optimal filtering' (Prentice-Hall, Englewood Cliffs, NJ, USA, 1979)
23 Bar-Shalom, Y., Fortmann, T.: 'Tracking and data association', mathematics in science and engineering' (Academic Press Professional Inc., San Diego, CA, USA, 1987), vol. 179
24 Julier, S.J., Uhlmann, J.K.: 'Unscented filtering and nonlinear estimation'. Proc. of the IEEE, 2004, vol. 92, no. 3, pp. 401–422
25 Gordon, N.J., Salmond, D.J., Smith, A.F.: 'Novel approach to nonlinear/non-Gaussian Bayesian state estimation'. IEE Proc. F (Radar and Signal Processing), April 1993, vol. 140, no. 2, pp. 107–113. IET Digital Library
26 Papi, F., Podt, M., Boers, Y., Battistello, G., Ulmke, M.: 'On constraints exploitation for particle filtering based target tracking'. Information Fusion (FUSION), Proc. 15th IEEE Int. Conf. on Information Fusion, 2012, pp. 455–462
27 Bar-Shalom, Y., Willett, P.K., Tian, X.: 'Tracking and data fusion: a handbook of algorithms' (YBS Publishing, Storrs, CT, USA, 2011)
28 Van Trees, H.L.: 'Detection, estimation, and modulation theory: radar-sonar signal processing and Gaussian signals in noise' (Krieger Publishing Co., Melbourne, FL, USA, 1992)